Supporting Information

Sockolosky et al. 10.1073/pnas.1208857109

SI Text

SI Materials and Methods. ***Materials.*** Ovalbumin, ampicillin, inulin-FITC, DAPI, and Terrific Broth (TB) were purchased from Sigma-Aldrich. The humanized anti-VEGF IgG1 antibody (bevacizumab) was obtained from the University of California, San Francisco (UCSF) medical center. Nickel Sepharose high-performance resin prepacked in 5-mL HiTrap columns (HisTrap FF), PD-10 desalting columns, and HiPrep 16/60 Sephacryl S-100 HR size exclusion chromatography (SEC) column were purchased from GE Healthcare. Complete EDTA-free protease inhibitor cocktail tablets, IPTG, and G418 were purchased from Roche Diagnostics. Dextran Cascade blue (10 kDa) and hygromycin B were from Invitrogen. All primers were purchased from IDT.

Cell culture. Madin–Darby canine kidney (MDCK) wild-type cells (purchased from the UCSF cell culture facility) were maintained in MEM supplemented with 10% FBS, 1% nonessential amino acids (NEAA), 1% L-glutamine, 1% sodium pyruvate, and 1% penicillin and streptomycin. B16F10 cells were maintained in MEM supplemented with 10% FBS, 1% NEAA, and 1% sodium pyruvate. All cells were maintained in a humidified environment at 37 °C and 5% CO_2.

Mammalian expression vectors. A plasmid encoding human neonatal FC receptor (hFcRn) linked to N terminus of enhanced YFP (EYFP) was generated by PCR amplification of human FcRn cDNA with primers to incorporate 5′ EcoRI and 3′ AgeI restriction sites along with DNA encoding a $[Gly_4Ser]_2$ linker separating the C terminus of hFcRn from the N terminus of EYFP. The resulting PCR product was restriction-cloned into the 5′ EcoRI and 3′ AgeI sites of the mammalian expression vector pEYFP–N1 (kindly provided by Alan Verkman, UCSF, San Francisco, CA). Human FcRn cDNA was obtained from OpenBiosystems and maintained in the vector pINCY. A plasmid encoding human β_2-microglobulin ($h\beta_2m$) was generated by PCR amplification of $h\beta_2m$ cDNA from the vector pCMV–SPORT6 (OpenBiosystems) followed by restriction cloning into the 5′ BamHI and 3′ XhoI sites of the mammalian expression vector pcDNA™3.1/Hygro (+) (kindly provided by Kathy Giacomini, UCSF, San Francisco, CA).

The plasmid encoding lysosomal-associated membrane protein 1 (LAMP1) linked to the C terminus of mTurquoise was generated by PCR amplification of LAMP1 from a cDNA library prepared from M28 human mesothelioma cells with primers designed to incorporate 5′ XhoI and 3′ BamHI restriction sites. The resulting PCR product was restriction-cloned into the 5′ XhoI and 3′ BamHI sites of the mammalian expression vector pmTurquoise-C1 (kindly provided by Kurt Thorn, UCSF, San Francisco, CA).

Escherichia coli expression vectors. The bacterial expression vector for mKate was generated as previously described (1). The genes encoding mKate modified at its C terminus with FcRn-binding polypeptide (FcBP) sequences were constructed by PCR amplification of mKate with primers designed to insert DNA encoding a cyclic or linear FcBP sequence (cyclic: QRFCTGHFGGLYPCNG; linear: QRFVTGHFGGLYPANG) separated from the C terminus of mKate by a flexible linker (GGGGS). The resulting PCR products were purified and restriction-cloned into the NdeI and BamHI restriction sites of the bacterial expression vector pET15b (Novagen). The solvent-exposed cysteine residues of mKate (Cys134 and Cys242) were mutated to serine with mutagenic oligonucleotides using the QuikChange Lightning mutagenesis kit (Agilent Technologies) to yield the final expression vectors pETmKc and pETmKl, corresponding to mKate modified at its C terminus with a cyclic or linear FcBP, respectively. The same method was used to create the expression vector for mKate modified at its N terminus with the cyclic FcBP sequence. The gene encoding mKate modified at its N and C termini with the cyclic FcBP sequence was generated by PCR amplification of C-terminal modified mKate from pETmKc with primers designed to add a N-terminal cyclic FcBP sequence. The resulting PCR product was cloned into pET15b, and the three amino acids between the thrombin cleavage site and start of the N-terminal cyclic FcBP sequence (Ser, His, Met) were deleted with a mutagenic oligonucleotide using the QuikChange Lightning mutagenesis kit to yield the vector pETmKnc. The pET15b vectors for expression of the Tyr-12 to His mutant of N-and-C-Term Cyclic FcBP mKate (pETmKncY286H) and N-Linear/C-Cyclic FcBP mKate (pETmKnLc) were created by mutagenesis of pETmKnc. All plasmids were confirmed by DNA sequencing. A complete list of primers used in this study is provided in Table S1 and the amino acid sequences of proteins used in this study are provided below.

Protein expression and purification. Expression of mKate and modified mKates was carried out in BL21-Codon Plus (DE3)–RIPL *E. coli* cells (Stratagene) harboring expression vectors described above. A 100-mL overnight *E. coli* culture was used to inoculate a 1-L culture of Terrific Broth containing 100 μg/mL ampicillin and 0.1 mM IPTG. Cells were cultured at 37 °C for 8 h and harvested by centrifugation. Cells were lysed by free-thaw and lysozyme treatment (1 mg/mL), followed by sonication and centrifugation. The supernatant-containing soluble proteins were purified by Ni^{2+} affinity chromatography followed by SEC on a HiPrep 16/60 Sephacryl S-100. The N-terminal polyhistidine tag was cleaved with thrombin (Amersham Biosciences) and removed by Ni^{2+} affinity chromatography. Purity was confirmed by SDS-PAGE.

Cell line generation and maintenance. MDCK wild-type cells were cotransfected with expression vectors encoding full-length hFcRn–EYFP and $h\beta_2m$ using Lipofectamine 2000 (Invitrogen), and selected first with 0.3 mg/mL hygromycin B (Invitrogen) followed by selection with 1.0 mg/mL G418 (Roche). Resistant colonies were evaluated by fluorescence microscopy to confirm expression of hFcRn–EYFP, selected, and expanded for further analysis. Propagated clones were further evaluated for binding of fluorescently labeled hIgG1 at pH 6 and colocalization with hFcRn–EYFP by fluorescence microscopy. Furthermore, the presence of hFcRn and $h\beta_2m$ mRNA was confirmed by RT-PCR. MDCK cells stably expressing $h\beta_2m$ were generated as described above to serve as a negative control. All stably transfected cells were maintained in MDCK wild-type media under constant drug selection (0.4 mg/mL G418 and/or 0.3 mg/mL hygromycin B).

mKate fluorescence in MDCK hFcRn–EYFP/hB2M cells after intracellular pH clamping. MDCK hFcRn–EYFP/$h\beta_2m$ cells seeded in a 12-well plate (250,000 cells per well) were washed twice in binding buffer [HBSS(+), pH 6] and incubated with either 25 μM mKate or 2.5 μM N-and-C-Term Cyclic FcBP for 1 h at pH 6, 37 °C, to permit cellular uptake. Cells were washed three times with cold binding buffer to remove unbound protein, trypsinized, and collected by centrifugation. The pH in all cellular compartments was

clamped by resuspending cells in high-K^+ solutions containing inhibitors and ionophores (50 mM Hepes, pH 7.4, or 50 mM acetic acid, pH 5 or pH 4, containing 140 mM KCl, 2 mM $CaCl_2$, 1 mM $MgCl_2$, 5 mM glucose, 100 nM bafilomycin A1, 10 μM nigericin, 10 μM valinomycin, and 10 μM CCCP) as described (2). After, pH clamp cells were analyzed by fluorescence-activated cell sorting (FACS) to determine differences in mKate mean fluorescent intensity (MFI) as a function of pH.

Fluorescent spectra measurements. All fluorescent spectra were measured on a Spex Fluorolog fluorometer (Horiba Jobin Yvon) with 5-nm excitation and emission slits. To compare fluorescent emission spectra between unmodified mKate or FcBP-modified mKates, proteins were diluted to 500 nM in D-PBS, excited at 588 nm. The emission spectra were then recorded. Quantification of protein samples by fluorometry was done by comparing unknown samples to a standard curve specific to each protein.

Fluorescence microscopy. Wide-field epifluorescence images of N-and-C-Term Cyclic FcBP mKate colocalization with hFcRn–EYFP in MDCK cells were obtained on a Nikon Eclipse Ti-E inverted microscope. MDCK hFcRn–EYFP/hβ_2m cells were pulsed with 1 μM protein at pH 6 for 1 h at 37 °C, washed, and imaged live on a temperature-controlled stage. The distribution of hFcRn–EYFP, N-and-C-Term Cyclic FcBP mKate, and LAMP1-mTurquoise in MDCK hFcRn–EYFP/hβ_2m cells was determined by transient transfection with the mammalian expression vector encoding LAMP1-mTurquoise as described. Cells were pulsed as described above, washed, and chased in HBSS, pH 7.4, at 37 °C for 1 or 4 h before imaging.

Confocal images were obtained on a Zeiss Axiovert 200 M inverted microscope equipped with a Yokogawa CSU10 spinning disc unit. Dextran pulse-chase studies were as follows: MDCK hFcRn–EYFP/hβ_2m cells were pulsed with 1 mg/mL of 10 kDa dextran-blue for 2 h at 37 °C, washed, and chased for 1 h at 37 °C in HBSS, pH 7.4. Cells were then pulsed with 1 μM of N-and-C-Term Cyclic FcBP mKate for 1 h at 37 °C, pH 6, washed, and chased for 1 h at 37 °C in HBSS, pH 7.4, prior to imaging.

All image analysis was performed using ImageJ (National Institutes of Health). Wide-field epifluorescent images in Fig. 3 were deconvoluted to remove out-of-focus light using the 2D parallel spectral deconvolution plugin.

Mass spectrometry. Mass spectrometry was performed by the Proteomics/Mass Spectrometry Laboratory at University of California, Berkeley. For liquid chromatography–tandem mass spectrometry (LC–MS/MS) analysis, proteins were digested in solution with LysC (Promega). The protein solution was adjusted to 8 M urea, subjected to carboxyamidomethylation of cysteines, and digested with LysC. The sample was then desalted using a C18 spec tip (Varian). A nano LC column was packed in a 100-μm inner diameter glass capillary with an emitter tip. The column consisted of 10 cm of Polaris C18 5-μm packing material (Varian). The column was loaded by use of a pressure bomb and washed extensively with buffer A (see below). The column was then directly coupled to an electrospray ionization source mounted on a Thermo-Fisher LTQ XL linear ion trap mass spectrometer. An Agilent 1200 HPLC equipped with a split line so as to deliver a flow rate of 30 nL/min was used for chromatography. Peptides were eluted using a linear gradient from 100% buffer A to 60% buffer B. Buffer A was 5% acetonitrile, 0.02% heptafluorobutyric acid (HBFA); buffer B was 80% acetonitrile, 0.02% HBFA. The programs SEQUEST and DTASELECT (3, 4) were used to identify peptides from a database consisting of the protein sequence plus a database of common contaminants using a partial tryptic search.

Statistical analysis. Comparison between two groups was analyzed for statistical significance using an unpaired, Student's *t* test (two-sided). Comparison between multiple groups was analyzed for statistical significance using a one-way ANOVA and Bonferroni posttest. All statistical analysis was performed in Prism 5 (GraphPad Software) on untransformed data.

Amino Acid Sequences of Protein Used in this Study. The FcBP sequence in each protein is in **boldfaced** letters. Mutants of the FcBP sequence are shown in ***bold faced and italic*** letters. The thrombin cleavage site is underlined.

mKate. MGSSHHHHHHSSGLVPRGSHMSELIKENMHMK-
LYMEGTVNNHHFKCTSEGEGKPYEGTQTMRIKV-
VEGGPLPFAFDILATSFMYGSKTFINHTQGIPDFFKQSF-
PEGFTWERVTTYEDGGVLTATQDTSLQDGCLIYNV-
KIRGVNFPSNGPVMQKKTLGWEASTEMLYPADGGLE-
GRSDMALKLVGGGHLICNLKTTYRSKKPAKNLKMPG-
VYYVDRRLERIKEADKETYVEQHEVAVAR-
YCDLPSKLGHK

C-terminal linear FcBP mKate. MGSSHHHHHHSSG*LVPRG*SHM-
SELIKENMHMKLYMEGTVNNHHFKCTSEGEGK-
PYEGTQTMRIKVVEGGPLPFAFDILATSFMYGSKT-
FINHTQGIPDFFKQSFPEGFTWERVTTYEDGGVL-
TATQDTSLQDGCLIYNVKIRGVNFPSNGPVMQKKTLG-
WEASTEMLYPADGGLEGRSDMALKLVGGGHLICNLKT-
TYRSKKPAKNLKMPGVYYVDRRLERIKEADKETYVEQ-
HEVAVARYCDLPSKLGHKGGGGS**QRFVTGHFGGLYPANG**

C-terminal cyclic FcBP mKate. MGSSHHHHHHSSG*LVPRG*SHM-
SELIKENMHMKLYMEGTVNNHHFKCTSEGEGK-
PYEGTQTMRIKVVEGGPLPFAFDILATSFMYGSKT-
FINHTQGIPDFFKQSFPEGFTWERVTTYEDGGVL-
TATQDTSLQDGSLIYNVKIRGVNFPSNGPVMQKKTLG-
WEASTEMLYPADGGLEGRSDMALKLVGGGHLICNLKT-
TYRSKKPAKNLKMPGVYYVDRRLERIKEADKETYVEQ-
HEVAVARYSDLPSKLGHKGGGGS**QRFCTGHFGGLYPCNG**

N-terminal cyclic FcBP mKate. MGSSHHHHHHSSG*LVPRG***QRF-**
CTGHFGGLYPCNGGGGGSSELIKENMHMKLY-
MEGTVNNHHFKCTSEGEGKPYEGTQTMRIKV-
VEGGPLPFAFDILATSFMYGSKTFINHTQGIPDFFKQSF-
PEGFTWERVTTYEDGGVLTATQDTSLQDGSLIYNV-
KIRGVNFPSNGPVMQKKTLGWEASTEMLYPADGGLE-
GRSDMALKLVGGGHLICNLKTTYRSKKPAKNLKMPG-
VYYVDRRLERIKEADKETYVEQHEVAVAR-
YSDLPSKLGHK

N-and-C-terminal cyclic FcBP mKate. MGSSHHHHHHSSG*LVP-*
*RG***QRFCTGHFGGLYPCNG**GGGGSSELIKENMHMKLY-
MEGTVNNHHFKCTSEGEGKPYEGTQTMRIKV-
VEGGPLPFAFDILATSFMYGSKTFINHTQGIPDFFKQSF-
PEGFTWERVTTYEDGGVLTATQDTSLQDGSLIYNV-
KIRGVNFPSNGPVMQKKTLGWEASTEMLYPADGGLE-
GRSDMALKLVGGGHLICNLKTTYRSKKPAKNLKMPG-
VYYVDRRLERIKEADKETYVEQHEVAVAR-
YSDLPSKLGHKGGGGS**QRFCTGHFGGLYPCNG**

N-and-C-terminal cyclic FcBP mKate Y286H. MGSSHHHHHHSSG-
*LVPRG***QRFCTGHFGGLYPCNG**GGGGSSELIKENMHMK-
LYMEGTVNNHHFKCTSEGEGKPYEGTQTMRIKV-
VEGGPLPFAFDILATSFMYGSKTFINHTQGIPDFFKQSF-
PEGFTWERVTTYEDGGVLTATQDTSLQDGSLIYNV-
KIRGVNFPSNGPVMQKKTLGWEASTEMLYPADGGLE-
GRSDMALKLVGGGHLICNLKTTYRSKKPAKNLKMPG-

VYYVDRRLERIKEADKETYVEQHEVAVAR-
YSDLPSKLGHKGGGGS**QRFCTGHFGGL*H*PCNG**

N-linear and C-cyclic FcBP mKate. MGSSHHHHHHSSG*LVPRG***Q-**
RF*V*TGHFGGLYP*A*NGGGGGSSELIKENMHMKLY-
MEGTVNNHHFKCTSEGEGKPYEGTQTMRIKV-
VEGGPLPFAFDILATSFMYGSKTFINHTQGIPDFFKQSF-
PEGFTWERVTTYEDGGVLTATQDTSLQDGSLIYNV-
KIRGVNFPSNGPVMQKKTLGWEASTEMLYPADGGLE-
GRSDMALKLVGGGHLICNLKTTYRSKKPAKNLKMPG-
VYYVDRRLERIKEADKETYVEQHEVAVAR-
YSDLPSKLGHKGGGGS**QRFCTGHFGGLYPCNG**

yCD-FcBP. MGSSHHHHHHSSG*LVPRG***QRFCTGHFGGLYP-**
CNGGGGGSVTGGMASKWDQKGMDIAYEEALLGY-
KEGGVPIGGCLINNKDGSVLGRGHNMRFQKGSATLH-
GEISTLENCGRLEGKVYKDTTLYTTLSPCDMCTGAIIMY-
GIPRCVIGENVNFKSKGEKYLQTRGHEVVVVD-
DERCKKLMKQFIDERPQDWFEDI-
GETGGGGS**QRFCTGHFGGLYPCNG**

hFcRn–YFP. MGVPRPQPWALGLLLFLLPGSLGAESHLSL-
LYHLTAVSSPAPGTPAFWVSGWLGPQQYLSYNSLR-
GEAEPCGAWVWENQVSWYWEKETTDLRIKEKLFLEAF-
KALGGKGPYTLQGLLGCELGPDNTSVPTAKFALN-
GEEFMNFDLKQGTWGGDWPEALAISQRWQQQDKAAN-
KELTFLLFSCPHRLREHLERGRGNLEWKEPPSMRLK-
ARPSSPGFSVLTCSAFSFYPPELQLRFLRN-
GLAAGTGQGDFGPNSDGSFHASSSLTVKSGDEHHYC-
CIVQHAGLAQPLRVELESPAKSSVLVVGIVIGVLLL-
TAAAVGGALLWRRMRSGLPAPWISLRGDDTGVLLPTP-
GEAQDADLKDVNVIPATA**GGGGSGGGGS**GPVATMVSK-
GEELFTGVVPILVELDGDVNGHKFSVSGEGEGDA-
TYGKLTLKFICTTGKLPVPWPTLVTTFGYGLQCFAR-
YPDHMKQHDFFKSAMPEGYVQERTIFFKDDGNYK-
TRAEVKFEGDTLVNRIELKGIDFKEDGNILGHKLEY-
NYNSHNVYIMADKQKNGIKVNFKIRHNIEDGSVQLAD-
HYQQNTPIGDGPVLLPDNHYLSYQSALSKDP-
NEKRDHMVLLEFVTAAGITLGMDELYK

hB2M. MSRSVALAVLALLSLSGLEAIQRTPKIQVYSRH-
PAENGKSNFLNCYVSGFHPSDIEVDLLKNGERIEK-
VEHSDLSFSKDWSFYLLYYTEFTPTEK-
DEYACRVNHVTLSQPKIVKWDRDM

1. Platt V, et al. (2010) Influence of multivalent nitrilotriacetic acid lipid-ligand affinity on the circulation half-life in mice of a liposome-attached His6-protein. *Bioconjugate Chem* 21:892–902.
2. Sonawane ND, Szoka FC, Verkman AS (2003) Chloride accumulation and swelling in endosomes enhances DNA transfer by polyamine-DNA polyplexes. *J Biol Chem* 278:44826–44831.
3. Eng JK, McCormack AL, Yates JR (1994) An approach to correlate tandem mass spectral data of peptides with amino acid sequences in a protein database. *J Am Soc Mass Spectrom* 5:976–989.
4. Tabb DL, McDonald WH, Yates JR (2002) DTASelect and contrast: Tools for assembling and comparing protein identifications from shotgun proteomics. *J Proteome Res* 1:21–26.

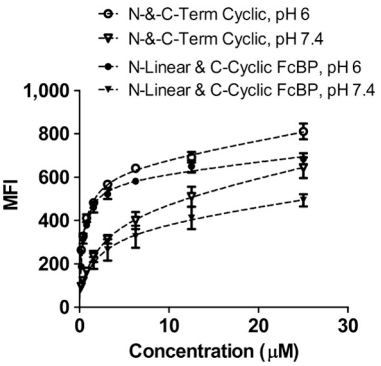

Fig. S1. Cellular accumulation of N-Linear and C-Cyclic FcBP mKate by FACS. Cellular accumulation of N-and-C-Term Cyclic FcBP mKate (blue) and N-Linear and C-Cyclic FcBP mKate mutant (green) showing similar accumulation in MDCK hFcRn–EYFP/hβ_2m cells at both pH 6 and pH 7.4. Cells were pulsed with increasing concentrations of protein for 1 h at 37 °C, washed, trypsinized, and analyzed by FACS. The data shown are the mean ($n = 3$), and error bars indicate SD. Dashed lines represent curve fit to a one-site total binding model in Prism.

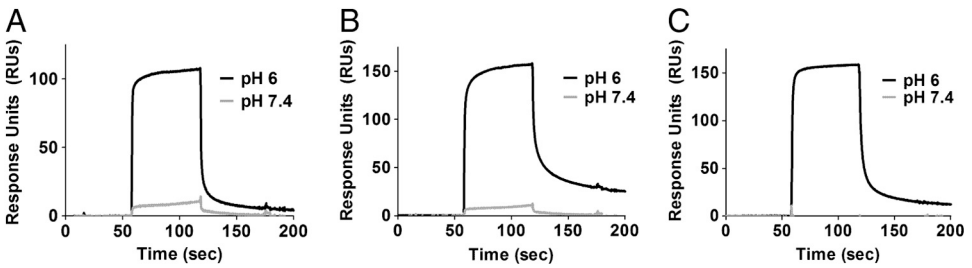

Fig. S2. FcBP-modified mKates exhibit pH-dependent binding to hFcRn by SPR. SPR sensograms of 12.5 μM N-Term Cyclic FcBP mKate (*A*), 5 μM N-and-C-Term Cyclic FcBP mKate (*B*), and 5 μM hIgG1 (*C*) binding to hFcRn at pH 6 (black line) and pH 7.4 (grey line). FcBP-modified mKate or hIgG1 was injected over immobilized hFcRn as described in *Materials and Methods*. FcRn immobilization density for the data shown is approximately 550 response units. All data were baseline-adjusted and reference cell-subtracted.

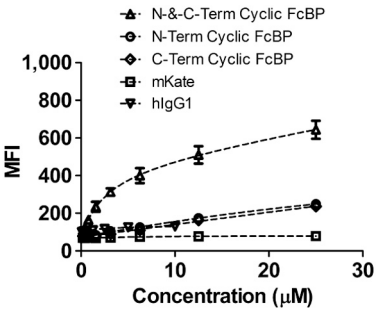

Fig. S3. Cellular accumulation of FcBP-modified mKates and labeled hIgG1 at pH 7.4. MDCK hFcRn–EYFP/hβ_2m cells were pulsed with increasing concentrations of protein for 1 h at 37 °C, washed, trypsinized, and analyzed by FACS. The data shown are the mean ($n = 3$), and error bars indicate SD. Dashed lines represent curve fit to a one-site total binding model in Prism.

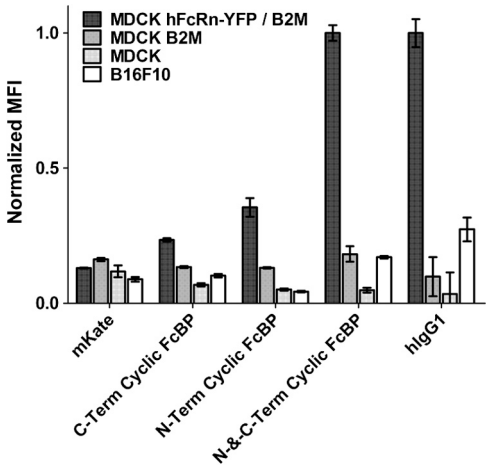

Fig. S4. Cellular accumulation of FcBP-modified mKates in various cell lines. Cells were pulsed with 1.5 μM of the specified protein for 1 h at pH 6 and 37 °C, washed, trypsinized, and analyzed for cellular accumulation by FACS. The MFI for modified and unmodified mKates was normalized to the maximum MFI for N-and-C-Term Cyclic FcBP mKate. hIgG1 was normalized to itself, given that the fluorescent intensity between the two fluorophores (mKate and TAMRA) are different.

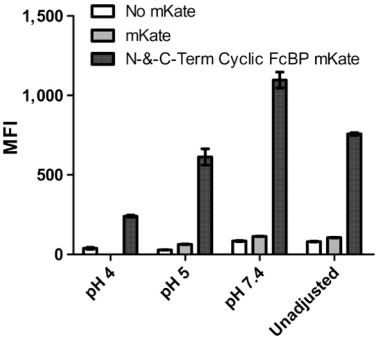

Fig. S5. Influence of pH clamping of MDCK hFcRn–EYFP/hB2M cells at pH 4, 5, or 7.4 on cell-associated mKate fluorescence. Cells were pulsed with 25 μM mKate or 2.5 μM N-and-C-Term Cyclic FcBP mKate for 1 h at pH 6 and 37 °C, washed, and trypsinized. The intracellular pH was clamped to either pH 4, 5, or 7.4 as described in *SI Materials and Methods*. The data shown are the mean ($n = 3$), and error bars indicate SD.

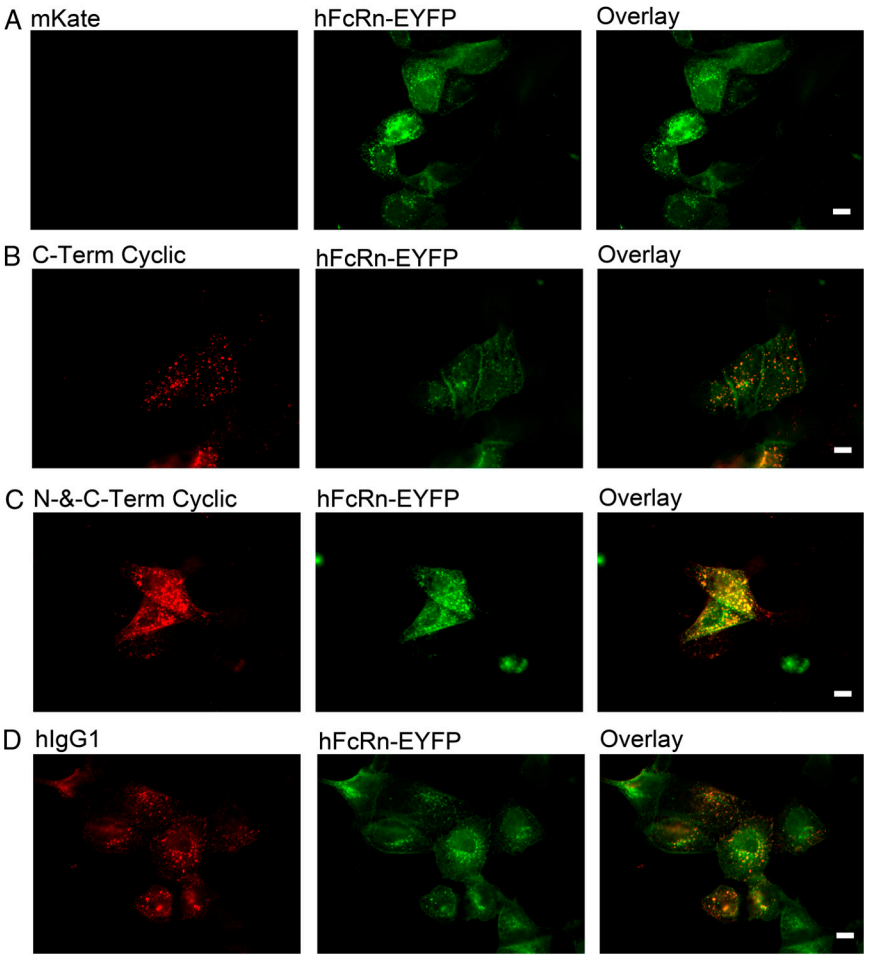

Fig. S6. Cyclic FcBP-modified mKates colocalize with hFcRn–EYFP in MDCK cells. Uptake of 5 μM mKate (*A*), 5 μM C-Term Cyclic FcBP mKate (*B*), 1 μM N-and-C-Term Cyclic FcBP mKate (*C*), or 1 μM Alexa-labeled hIgG1 (*D*) by MDCK cells transfected with hFcRn–EYFP and hβ2m at 37 °C. Cells were pulsed for 1 h with protein at pH 6, washed, fixed, and imaged. The same imaging and processing conditions were used for all images. mKates and Alexa-labeled hIgG1 are pseudocolored in red and hFcRn–EYFP in green. Yellow indicates colocalization between mKates (red) and hFcRn (green). Scale bars, 10 μm.

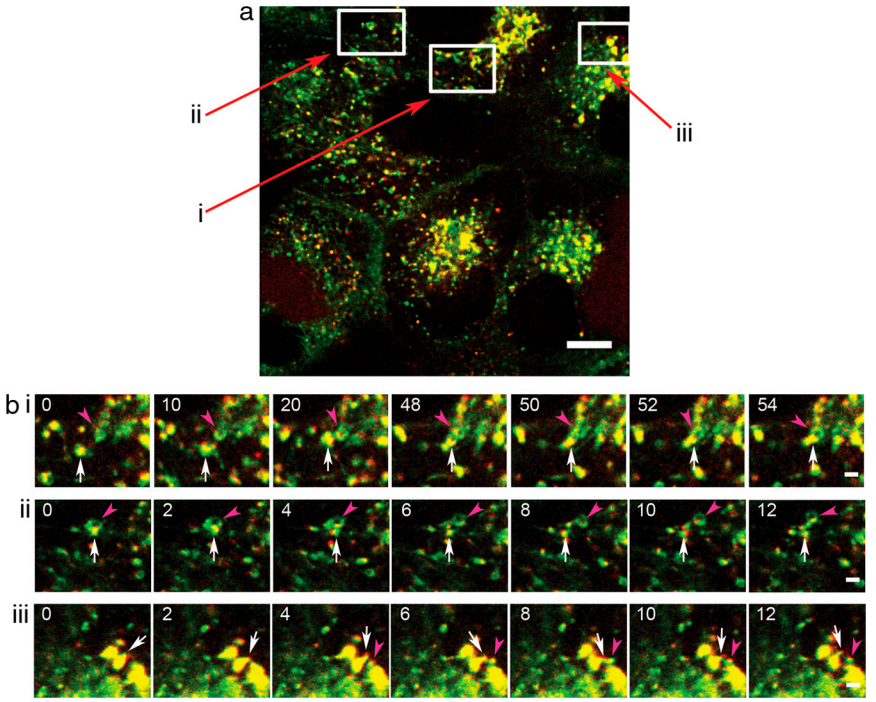

Fig. S7. N-and-C-Term Cyclic FcBP mKate is trafficked by hFcRn–EYFP in MDCK cells. MDCK hFcRn–EYFP/hβ_2m cells were pulsed with 1 μM of N-and-C-Term Cyclic FcBP mKate for 1 h at 37 °C and pH 6, washed, and imaged immediately on a stage preheated to 37 °C. (*A*) Full-size confocal image depicting areas presented as cropped images in (*B*, *i–iii*). (*B*) Confocal images depicting (*i*) endosomal fusion, (*ii*) vesicle budding, and (*iii*) tubule-mediated transfer events. The arrow in *B*, *i*, marks a FcRn–YFP and N-and-C-Term Cyclic FcBP mKate-positive compartment that eventually fuses with the FcRn–YFP-positive vesicle marked by the pink arrowhead. The arrow in *B, ii*, marks a subset of an endosomal vesicle (pink arrowhead) that eventually buds and traffics away from the parent FcRn–YFP–positive vesicle (pink arrowhead). The arrow in *B, iii*, marks a FcRn–YFP and N-and-C-Term Cyclic FcBP mKate-positive compartment in which a tubule rapidly extends, makes contact with another FcRn–YFP compartment (pink arrowhead), and retracts. Time (s) of each frame relative to the first frame is shown in the top left corner of each image. Images were pseudocolored as follow: green depicts FcRn–YFP; red depicts N-and-C-Term Cyclic FcBP mKate; and yellow indicates colocalization of FcRn–YFP and N-and-C-Term Cyclic FcBP mKate. Scale bars, 10 μm.

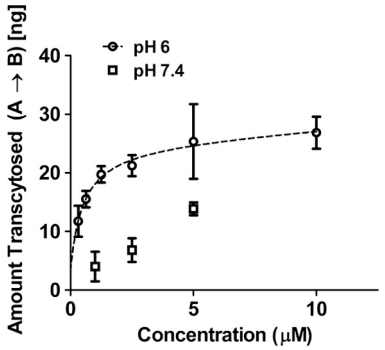

Fig. S8. Dose-dependent transcytosis of N-and-C-Term Cyclic FcBP mKate across MDCK hFcRn/B2M cell monolayers. Transcytosis of N-and-C-Term Cyclic FcBP mKate in the apical to basolateral direction after a 2-h continuous incubation with increasing concentrations of protein in the apical chamber equilibrated to either pH 6 or pH 7.4. The basolateral chamber was equilibrated to pH 7.4 in both cases. The data shown for each panel are the mean ($n = 3$), and error bars indicate SD. The dashed line represents a curve fit to a one-site total binding model in Prism.

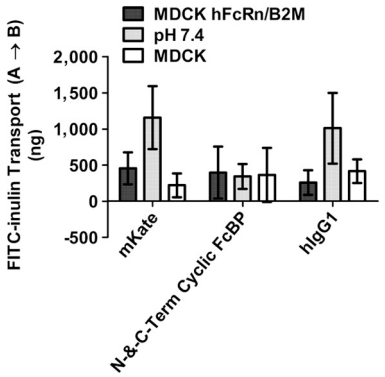

Fig. S9. Transport of FITC-inulin across MDCK cell monolayers. The paracellular transport probe FITC-inulin (4 μg/mL) was coincubated with each protein during transcytosis experiments to ensure the integrity of cell monolayers across transwells. The amount of FITC-inulin transported is similar across transwells indicating that differences in protein transport are not caused by defects in the cell monolayer. The data shown are mean ($n = 3$), and error bars indicate SD.

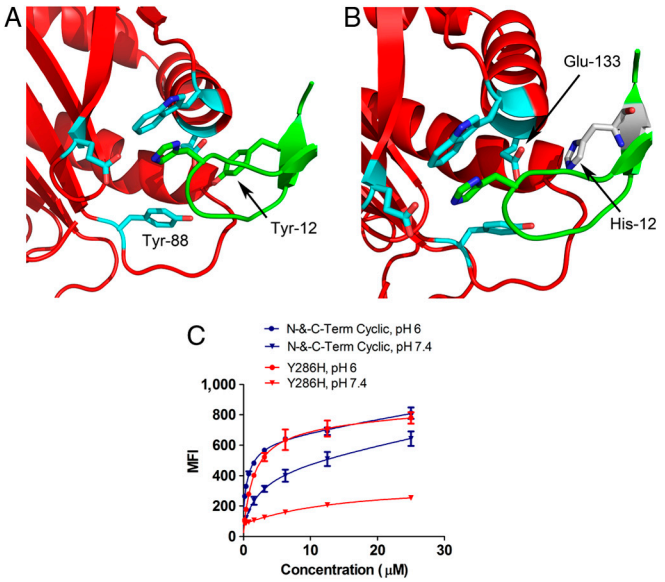

Fig. S10. Tyr-12 to His mutation of the cyclic FcBP improved pH-dependent binding to hFcRn. (*A*) Crystal structure of the cyclic FcBP (green) in complex with hFcRn (red backbone and blue side chains). (*B*) Crystal structure of the cyclic FcBP in complex with hFcRn, showing the Tyr-12 to His mutation and its proximity to Glu-133 of hFcRn. The images in *A* and *B* were generated from the published crystal structure (1) using PyMOL (Protein Data Bank ID: 3M17). (*C*) Cellular accumulation of N-and-C-Term Cyclic FcBP mKate (blue) and N-and-C-Term Cyclic FcBP mKate Y286H mutant (red), showing reduced accumulation in MDCK hFcRn–EYFP/hβ_2m cells at pH 7.4 with no effect on accumulation at pH 6. Cells were pulsed with increasing concentrations of protein for 1 h at 37 °C, washed, trypsinized, and analyzed by FACS. The data shown are the mean ($n = 3$), and error bars indicate SD. Solid lines represent curve fit to a one-site total binding model in Prism.

1 Mezo AR, Sridhar V, Badger J, Sakorafas P, Nienaber V (2010) X-ray crystal structures of monomeric and dimeric peptide inhibitors in complex with the human neonatal Fc receptor, FcRn. *J Biol Chem* 285:27694–27701.

Table S1. List of primers used in this study

Protein	Primer pair	Restriction site
hFcRn–YFP	F = 5′-AAG CTT CGA ATT CCT CAG CAT GGG GTC-3′ R = 5′-GCG ACC GGT CCG GAC CCC CCC CCC CCG GAC CCC CCC CCC CCG GCG GTG GCT GGA ATC ACA-3′	EcoRIAgeI
hB2M	F = 5′-CGA GCT CGG ATC CGC CGA GAT GTC TCG CTC CGT GG-3′ R = 5′-CTC TAG ACT CGA GTT ACA TGT CTC GAT CCC ACT TAA C-3′	BamHIXhoI
hLAMP1-mTurquoise	F = 5′-GATCTCGAGCGCCACCATGGCGGCCCCCGGCAGC-3′ R = 5′-GGTGGATCCGGGATAGTCTGGTAGCCTGC-3′	XhoIBamHI
C-Term Cyclic FcBP mKate	F = 5′-CGGCAGCCATATGTCTGAACTGATCA-3′ R = 5′-GCA GCC GGA TCC TTA GCC GTT GCA CGG ATA CAG GCC GCC AAA ATG GCC GGT GCA AAA GCG CTG CGA GCC GCC GCC GCC TTT ATG GCC CAG TTT AGA-3′	NdeIBamHI
C-Term Linear FcBP mKate	F = 5′-CGGCAGCCATATGTCTGAACTGATCA-3′ R = 5′-GCA GCC GGA TCC TTA GCC GTT CGC CGG ATA CAG GCC GCC AAA ATG GCC GGT CAC AAA GCG CTG CGA GCC GCC GCC GCC TTT ATG GCC CAG TTT AGA-3′	NdeIBamHI
N-Term Cyclic FcBP mKate	F = 5′-CAG CCA TAT GCA ACG TTT CTG TAC CGG TCA CTT CGG TGG TCT GTA CCC GTG TAA TGG TGG TGG TGG TGG TTC GTC TGA ACT GAT CAA AGA-3′ R = 5′-GCCGGATCCTTATTTATGGCCCAGTT-3′	NdeIBamHI
N-and-C-Term Cyclic FcBP mKate	F = 5′-CAG CCA TAT GCA ACG TTT CTG TAC CGG TCA CTT CGG TGG TCT GTA CCC GTG TAA TGG TGG TGG TGG TGG TTC GTC TGA ACT GAT CAA AGA-3′ R = 5′-GCA GCC GGA TCC TAG CCG TTG-3′	NdeIBamHI
N-and-C-Term Cyclic FcBP mKate Y286H mutagenesis	5′-ATT TTG GCG GCC TGC ATC CGT GCA ACG GC-3′	-
N-Linear and C-Cyclic FcBP mKate C22V mutagenesis	5′-CGC GGC CAA CGT TTC GTT ACC GGT CAC TTC GG-3′	-
N-Linear and C-Cyclic FcBP mKate C32A mutagenesis	5′-GGT GGT CTG TAC CCG GCT AAT GGT GGT GGT GG-3′	-
N-terminal SHM deletion mutagenesis	5′-TGG TGC CGC GCG GCC AAC GTT TCT GTA C-3′	-
qPCR hFcRn forward	5′-CCT GGC TTT TCC GTG CTT AC-3′	-
qPCR hFcRn reverse	5′-TTT GAC TGT TAG TGA CGA CGA G-3′	-
qPCR hB2M rorward	5′-GAG GCT ATC CAG CGT ACT CCA-3′	-
qPCR hB2M reverse	5′-CGG CAG GCA TAC TCA TCT TTT-3′	-